A Novel Binuclear [CuSMo] Cluster at the Active Site of Carbon Monoxide Dehydrogenase: Characterization by X-ray Absorption Spectroscopy†

Manuel Gnida,‡ Reinhold Ferner,§ Lothar Gremer,§ Ortwin Meyer,§,|| and Wolfram Meyer-Klaucke*,‡

European Molecular Biology Laboratory (EMBL), Outstation Hamburg at DESY, Notkestrasse 85, D-22603 Hamburg, Germany, Department of Microbiology and Bayreuth Center of Molecular Biosciences (BZMB), University of Bayreuth, Universitätsstrasse 30, D-95440 Bayreuth, Germany

Received July 25, 2002; Revised Manuscript Received October 14, 2002

ABSTRACT: The structurally characterized molybdoenzyme carbon monoxide dehydrogenase (CODH) catalyzes the oxidation of CO to CO_2 in the aerobic bacterium *Oligotropha carboxidovorans*. The active site of the enzyme was studied by Mo− and Cu−K-edge X-ray absorption spectroscopy. This revealed a bimetallic [$Cu^{I}SMo^{VI}(=O)_2$] cluster in oxidized CODH which was converted into a [$Cu^{I}SMo^{IV}(=O)OH_{(2)}$] cluster upon reduction. The Cu···Mo distance is 3.70 Å in the oxidized form and is increased to 4.23 Å upon reduction. The bacteria contain CODH species with the complete and functional bimetallic cluster along with enzyme species deficient in Cu and/or bridging S. The latter are precursors in the posttranslational biosynthesis of the metal cluster. Cu-deficient CODH is the most prominent precursor and contains a [$HSMo(=O)OH_{(2)}$] cluster. Se−K-edge X-ray absorption spectroscopy demonstrates that Se is coordinated by two C atoms at 1.94−1.95 Å distance. This is interpreted as a replacement of the S in methionine residues. In contrast to a previous report [Dobbek, H., Gremer, L., Meyer, O., and Huber, R. (1999) *Proc. Natl. Acad. Sci. U.S.A. 96*, 8884−8889] Se was not identified in the active site of CODH.

Carbon monoxide dehydrogenase (CODH)[1] from the aerobic bacterium *Oligotropha carboxidovorans* is a copper- and selenium-containing molybdo−iron−sulfur flavoprotein and, according to its sequence, belongs to the family of molybdenum hydroxylases (*1*). It is the key enzyme in the utilization of CO by *O. carboxidovorans*, when CO is the sole source of carbon and energy (*2*), and catalyzes the oxidation of CO according to the equation $CO + H_2O \rightarrow CO_2 + 2H^+ + 2e^-$ (*3*). CODH from *O. carboxidovorans* is composed of an 88.7 kDa molybdoprotein (L subunit), a 30.2 kDa flavoprotein (M subunit), and a 17.8 kDa iron−sulfur protein (S subunit) and forms dimers of LMS heterotrimers (*4*). The molybdoprotein contains one molecule of the molybdenum cofactor, which is a 1:1 mononuclear complex of molybdopterin−cytosine dinucleotide (MCD) and a Mo, carrying a single S-substituent and two O-substituents (*5*). The flavoprotein contains one molecule of noncovalently bound flavin adenine dinucleotide (FAD). The iron−sulfur protein carries two [2Fe-2S] clusters which can be distinguished by electron paramagnetic resonance (EPR) spectroscopy (*6*). CO oxidation takes place at the molybdenum site. The electrons produced are transferred via the iron−sulfur clusters to FAD where they leave the enzyme (*6*).

In a previous crystallographic paper the active site of a CODH preparation with a specific activity of 6.6 units mg^{-1} has been modeled as a Mo coordinated by three O-substituents and complexed by the enedithiolates of MCD along with a SeH group attached to the Sγ of Cys^{388} (*4*). In a subsequent crystallographic model, the active site of an enzyme preparation with a specific activity of 23 units mg^{-1} has been refined as a Mo coordinated by the enedithiolate group of an MCD (Mo−S distances 2.3 and 2.4 Å), two oxo groups (1.7 Å), and a sulfido ligand (2.3 Å) bridging the Mo ion and an electron dense atom (3.7 Å), which is covalently bound to the Sγ of Cys^{388}. This electron dense atom was modeled as a Se atom (*5*). The presence of a S ligand at the Mo became also apparent from the reaction of CODH with cyanide which inactivates the enzyme and leads to the formation of thiocyanate and a desulfo EPR spectrum (*5*). Recent crystallographic studies on a 23 units mg^{-1} CODH enzyme preparation further substantiated the presence of a cyanolyzable S ligand at the Mo and identified by multiple wavelength anomalous dispersion (MAD) experiments the active site to be composed of a binuclear Cu- and Mo-containing center in which the S ligand bridges both metals (*7*). The presence of Se in the active site as proposed earlier (*4*, *5*) could not be confirmed.

† M.G. was financially supported by the German Ministry of Education and Research (BMBF, Contract 05 SN8 FLA7). O.M. acknowledges a grant (Me 732/8-1) from the Deutsche Forschungsgemeinschaft (DFG), Bonn, Germany.

* To whom correspondence should be addressed. Tel: ++49-40-89902-124. Fax: ++49-40-89902-149. E-mail: Wolfram@embl-hamburg.de.

‡ European Molecular Biology Laboratory.

§ Department of Microbiology, University of Bayreuth.

|| Bayreuth Center of Molecular Biosciences, University of Bayreuth.

[1] Abbreviations: CODH, carbon monoxide dehydrogenase; MCD, molybdopterin−cytosine dinucleotide; FAD, flavin adenine dinucleotide; EPR, electron paramagnetic resonance; units mg^{-1}, units per milligram; MAD, multiple anomalous dispersion; XAS, X-ray absorption spectroscopy; EXAFS, extended X-ray absorption fine structure; INT, 1-phenyl-2-(4-iodophenyl)-3-(4-nitrophenyl)-2*H*-tetrazolium chloride; MPMS, 1-methoxyphenazine methosulfate; CODH-H/M/L, CODH with high, medium, and low specific activity; SDS, sodium dodecyl sulfate; PAGE, polyacrylamide gel electrophoresis; ICP-AES, inductively coupled plasma atomic emission spectroscopy; XANES, X-ray absorption near edge structure; BCA, 2,2′-bis(quinoline)-4,4′-dicarboxylic acid.

10.1021/bi026514n CCC: $25.00
Published on Web 12/10/2002

X-ray absorption spectroscopy (XAS) allows the selective and precise investigation of the coordination environments of elements and yields structural information about the active sites of metalloproteins at subatomic resolution (*8*, *9*). In the present paper XAS is employed to investigate the structure of the heteronuclear metal cluster in the active site of CODH. The enzyme has been studied in the presence and absence of its substrate CO and in mixtures of the functional species with nonfunctional forms which are likely precursors in the posttranslational processing of the active site, as is discussed below. We have recorded the extended X-ray absorption fine structures (EXAFS) of the K-absorption edges of Mo, Cu, and Se and combined the data for the different elements in a multiple K-edge analysis. Thereby, the active site of CODH is characterized as a novel flexible binuclear [CuSMo] cluster in which a S bridges the two metals and the Cu occupies the position where formerly Se has been modeled. It seems that the Se present in CODH replaces part of the S in the total number of 94 methionine residues present in the enzyme.

MATERIALS AND METHODS

CODH from *O. carboxidovorans* was isolated and purified as described previously (*6*). The oxidation of CO by the enzyme was detected photometrically with 1-phenyl-2-(4-iodophenyl)-3-(4-nitrophenyl)-2*H*-tetrazolium chloride (INT) and 1-methoxyphenazine methosulfate (MPMS) as artificial electron acceptors (*10*). Specific enzyme activities are given in units per milligram (units mg^{-1}). One unit is defined as the enzyme activity which corresponds to the amount of 1 μmol of CO oxidized per minute at 30 °C. The preparations of CODH used (CODH-H, high activity, 23 units mg^{-1}; CODH-M, medium activity, 16 units mg^{-1}; CODH-L, low activity, 4 units mg^{-1}) were homogeneous according to native and sodium dodecyl sulfate (SDS)−polyacrylamide gel electrophoresis (PAGE) analysis. Enzyme concentrations were determined by employing an extinction coefficient (ϵ_{450}) of 72 mM^{-1} cm^{-1} (*11*).

For analyses of cyanolyzable sulfur CODH preparations (3 mg mL^{-1}) were treated for 20 h with 5 mM potassium cyanide under 100% argon, and protein was removed by ultrafiltration (30 kDa cutoff). Thiocyanate in the ultrafiltrate was colorimetrically analyzed as $Fe(SCN)_3$ (*12*). Cu was determined by inductively coupled plasma atomic emission spectroscopy (ICP-AES).

For XAS measurements, 75 μL of enzyme solution (in 50 mM HEPES buffer, pH 7.2) was filled into sample cells of HESAR glass covered with Kapton windows. The cells were sealed and kept at temperatures below 194 K. CO-treated samples were prepared by incubating solutions of oxidized CODH with pure CO under anoxic conditions for at least 4 h at room temperature, prior to filling them into CO-flushed sample cells.

The powder sample of selenomethionine was prepared by mixing 20 mg of seleno-L-methionine with 77 mg of boron nitride to avoid "thickness effects" (*13*) in the X-ray absorption spectrum. The mixture was pasted homogeneously into a sample cell similar to the one described above.

XAS data were collected at DESY (Hamburg, Germany) at the EMBL bending magnet EXAFS beam line D2 using Si(111) and Si(220) double monochromators for measurements at the Se−/Cu−K-edges and at the Mo−K-edge, respectively. The maximum positron current of the DORIS storage ring (positron energy 4.5 GeV) was about 145 mA. Absolute energy calibration of the spectra was achieved by recording Bragg reflections of a static Si(220) crystal in back-reflection geometry (*14*). The Se−K-edge spectrum of CODH-H was calibrated with respect to the corresponding CODH-L spectrum. The sample cells were mounted in a two-stage Displex cryostat (modified Oxford instruments) and kept at about 30 K. The X-ray absorptions of enzyme samples were recorded as Mo−, Cu−, and Se−K_α fluorescence excitation spectra using a Canberra 13-element solid-state detector, whereas the powder sample of selenomethionine was observed in absorption mode. To obtain comparable statistics, a different number of scans was collected and averaged for each sample. Data reduction, such as background removal and extraction of the EXAFS, was achieved with the EXPROG program package (*15*), assuming K-edge positions of $E_{0,Cu}$ = 8979 eV, $E_{0,Se}$ = 12658 eV, and $E_{0,Mo}$ = 20002 eV. EXAFS data (55−630/65−590/50−750 for Cu/Se/Mo) were analyzed using the refinement program EXCURV98 (*16*).

RESULTS AND DISCUSSION

Se−K-Edge EXAFS Excludes the Presence of Se at the Active Site of CODH. The presence of Mo and Se with an interatomic distance of 3.7 Å at the active site of CODH has been previously claimed (*4*, *5*). To generate confirmatory evidence at the subatomic level, we have examined the coordination environment of Se in CODH by Se−K-edge XAS. The Se−K-edge EXAFS (Figure 1A) and the Fourier transforms (Figure 1B) of CODH preparations of high (CODH-H) and low (CODH-L) activity (see Materials and Methods) were very similar. If Se would be part of the active site, Se should be coordinated by S donors (*4*, *5*). In contrast, fits assuming S backscattering contributions led to unrealistically short Se−S distances of 2.05 Å and large shifts in the energy threshold E_F [see manual of EXCURV98 (*16*)] compared to selenomethionine, which is inconsistent with the identical edge positions (data not shown). Thus these models are excluded. However, the data could be fitted by two C atoms at a distance of 1.95 Å (CODH-H) or 1.94 Å (CODH-L), which is indistinguishable within the numerical uncertainties. The observed Se−C distances are in excellent agreement with the Se−C distance in selenomethionine (1.96 Å; legend of Figure 1). The postulated carbon coordination of the Se is obvious from the similarity of the EXAFS spectra of CODH and selenomethionine (Figure 1). The contributions of the three nearest C atoms in the environment of Se in selenomethionine were extracted from the absorption spectrum of authentic selenomethionine. These carbon contributions (Figure 1, light gray curve) reproduce the experimental data of both CODH preparations (Figure 1, black and dark gray curves). These data suggest that Se in CODH-H, as well as in CODH-L, is coordinated by two C atoms in the first shell and that Se replaces part of the S in several of the 94 methionine residues present in CODH. The comparison of the experimental Se−K-edge spectra (Figure 1, solid lines) with a simulated Mo contribution assuming a Mo−Se binuclear center (Figure 1, dashed line) argues against the presence of a Mo within a distance of 4 Å in either CODH-H or CODH-L.

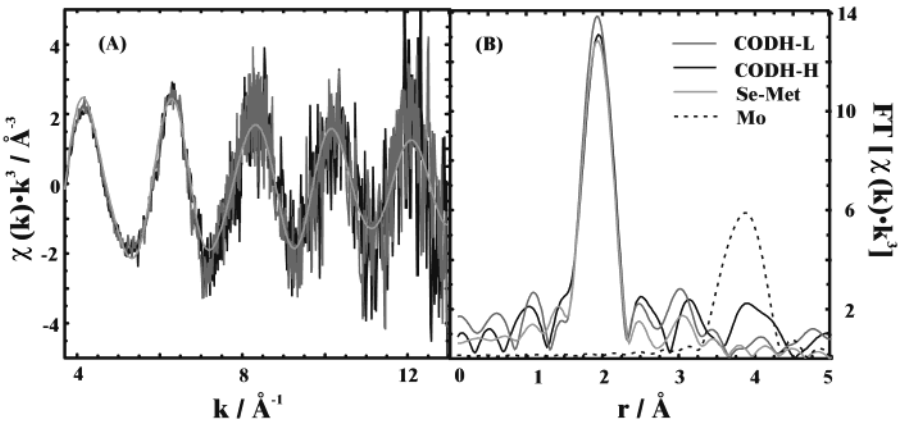

FIGURE 1: Se−K-edge EXAFS (A) and Fourier transforms (B) of oxidized CODH-H (solid black curve) and CODH-L (dark gray curve). The model for the backscattering contributions of the three nearest C atoms in selenomethionine (light gray curve, Se-Met) is also depicted. It was deduced from the EXAFS of a powder sample of selenomethionine (not shown): two C atoms at a distance $r = 1.96$ Å and one C atom at $r = 2.93$ Å. The dashed curve (black, Mo) represents a simulated Mo backscattering contribution at 3.80 Å (Debye−Waller parameter $2\sigma^2 = 0.007$ Å^2). The parameters were chosen in such a way that, in the Mo−K-edge spectrum shown in Figure 2B, a Se contribution would match the respective peak. Abbreviations: χ, EXAFS amplitude; *k*, photoelectron wavenumber; *r*, distance; FT, Fourier transform amplitude.

The exclusive carbon coordination instead of the expected ligation by S donors along with the absence of a Mo backscattering contribution Se···Mo excludes Se from being a constituent of the CODH active site irrespective of the activity of the enzyme preparation. In addition, the Mo and Cu EXAFS data presented below clearly show that Cu is at the position that formerly was assigned to Se. Moreover, the Se−K-edge positions for the three samples (CODH-H, CODH-L, and selenomethionine) coincide (data not shown). As discussed by Eidsness et al., the Se absorption edge shifts to lower energies compared to that of selenomethionine if Se is bound to higher Z elements than C (*17*). This also supports our interpretation that, in the investigated enzyme samples, Se is coordinated by two C atoms in the first shell and that no heavier atoms are present in the direct environment of selenium. In summary, these results correct a previous report in which a Se atom has been modeled 3.7 Å away from the Mo (*4*, *5*) and is in agreement with a reinvestigation of the crystallographic study of the CODH active site by MAD measurements at atomic resolution, EPR, and chemical analyses which identify a Cu at the position where formerly the Se has been modeled (*7*). The previous interpretation of this anomalous scatterer as Se (*4*, *5*) was misled by an inappropriate selection of the low-energy wavelength [$\lambda = 1.732$ Å (*4*)], thereby including the absorption edges of several other elements inclusive Cu. Although a fluorescence scan showed the presence of Se in CODH crystals, reinvestigation could not identify a single Se site in the anomalous difference Fourier maps (*7*).

Mo−K-Edge EXAFS of CODH-H Identifies a S Atom at a Distance of 2.29 Å to the Mo. According to the Mo−K-edge EXAFS spectrum of CODH-H (Figure 2A) and the corresponding Fourier transform (Figure 2B), Mo is coordinated by five ligands: a S at a distance of 2.29 Å, two additional S at 2.50 Å, and two O at 1.74 Å [Table 1 (I)]. The S at short distance was shown to be an inorganic, cyanolyzable S ligand, which reacts with cyanide, yielding thiocyanate and giving rise to a rhombic desulfo-inhibited type of Mo EPR signal (*5*). Inclusion of an additional O at 3.45 Å leads to a slight improvement of the fit [*R*-factor (*16*) decreases by 1.2%]. This contribution appears at a distance indicative for the presence of the highly conserved glutamate residue (Glu^{763}) also identified by X-ray crystallography (*4*, *5*, *7*) as well as in the EXAFS of CO-incubated CODH-H (see Table 2).

The Mo−K-edge position for oxidized CODH-H, defined as the first inflection point of the rising edge, is at 20003.0 eV (uncertainty about 0.5 eV) and corresponds to a formal metal oxidation state of Mo^{VI} (Figure 3A). This assignment is in accordance with EPR measurements performed at 120 K showing an EPR-silent Mo state (data not shown).

Cu−K-Edge and Mo−K-Edge EXAFS Indicates a SCuS Residue Proximal to the Mo. Previous studies reported 1.54 mol of Cu (*18*) and, more recently, 1.96 mol of Cu (*7*) per mole of CODH. In the absence of a known function of the metal in the enzyme, the Cu has so far been interpreted as an unspecific contamination. However, the proportionality between the CODH activities and the Cu contents shown in Figure 4 refers to a crucial function of the metal in catalysis. Therefore, we studied the coordination environment of Cu in CODH-H. The Cu−K-edge EXAFS spectrum of CODH-H (Figure 2C) and the corresponding Fourier transform (Figure 2D) show backscattering contributions of two S at a distance of 2.18 Å to the Cu [Table 1 (I)]. The peak at 3.69 Å in the Fourier transform could be reproduced by assuming a Mo at the indicated distance [Figure 2D, Table 1 (I)]. A corresponding Cu contribution is present in the Mo−K-edge spectrum at a distance of 3.70 Å from the Mo [Figure 2B, Table 1 (I)]. Thus, a Cu atom coordinated by two S is present at the position where a Se had formerly been modeled (*4*, *5*). According to the studies of Kau et al. (*19*), the intensity of the X-ray absorption near-edge structure (XANES) peak at 8984 eV in the Cu−K-edge identifies Cu as two-coordinate Cu^{I} in a nonlinear conformation (Figure 3B). Another sensitive indicator for the Cu coordination in cuprous−thiolate species is the Cu−S distance (*20*). The value of 2.18 Å observed in CODH-H agrees with digonal S−Cu^{I}−S.

The Active Site of Oxidized CODH-H Contains a Binuclear [Cu^{I}SMo^{VI}(=O)$_2$] Cluster. The separate structural models for the Mo and Cu coordination presented above were combined in a simultaneous refinement (*21*) of their EXAFS data, leading to a more accurate determination of the active site

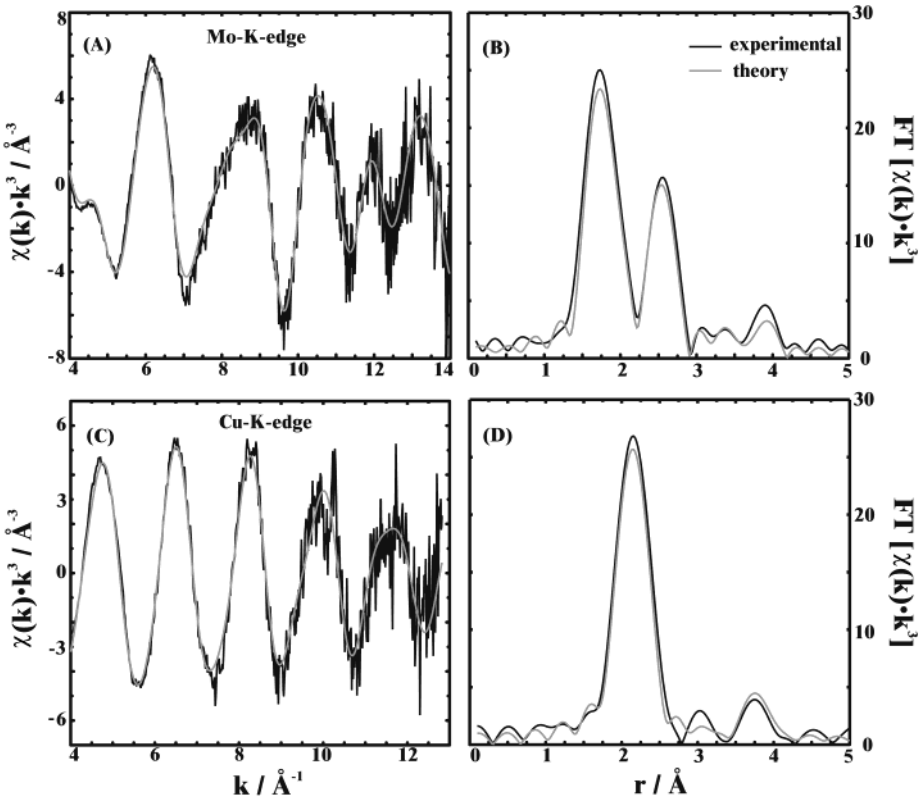

FIGURE 2: Mo−K-edge (A) and Cu−K-edge (C) EXAFS and Fourier transforms (B, D) for oxidized CODH-H. Experimental data are shown by black lines; calculated spectra are represented by gray curves. Parameters are listed in Table 1 (II). For abbreviations see Figure 1.

Table 1: EXAFS Refinement Parameters for Oxidized CODH-H[a]

model	atom	*N*	*r*/Å	$2\sigma^2$/Å^2	E_F[b]/eV	*R*[c]/%
(I)	Mo═O	2	1.737(4)	0.004(1)[d]	−13(2)	28.7
Mo−K-edge	Mo−S	1	2.289(5)	0.005(1)[d]		
	Mo−S	2	2.498(4)	0.005(1)[d]		
	Mo−O	1	3.453(27)	0.004(1)[d]		
	Mo···Cu	1	3.698(12)	0.010(3)		
Cu−K-edge	Cu−S	2	2.176(5)	0.008(1)	−10(1)	31.0
	Cu···Mo	1	3.688(13)	0.015(3)		
(II)	Mo═O	2	1.738(4)	0.004(1)[d]	Mo: −13(2)	29.2
simultaneous	Mo−S	1	2.289(5)	0.005(1)[d]	Cu: −11(1)	
refinement	Mo−S	2	2.499(4)	0.005(1)[d]		
	Mo−O	1	3.445(23)	0.004(1)[d]		
	Mo···Cu	1	3.703(10)	0.014(2)		
	Cu−S	2	2.179(5)	0.008(1)		

[a] *N*, number of atoms; *r*, distance; $2\sigma^2$, Debye−Waller parameter; E_F, Fermi energy; *R*, *R*-factor. Values in parentheses represent the numerical precision (twice the standard deviation) of the last digit. The accuracy of the distance determination by EXAFS is 0.01−0.02 Å. We therefore give only two decimals in the text. [b] The Fermi energy is related to the energetic position of the absorption edge [see manual of EXCURV98 (*16*)]. [c] The *R*-factor reflects the goodness of the fit and is defined in ref *16*. [d] Constrained to have the same value during refinement for identical atom types.

Table 2: EXAFS Refinement Parameters for CO-Incubated CODH-H[a]

model	atom	*N*	*r*/Å	$2\sigma^2$/Å^2	E_F[b]/eV	*R*[c]/%
Mo−K-edge	Mo═O	1.3(1)	1.700(5)	0.005(1)[d]	−12(2)	24.0
	Mo−O	0.7[e]	2.164(32)	0.005(1)[d]		
	Mo−S	2	2.354(5)	0.003(2)[d]		
	Mo−S	1	2.459(14)	0.003(2)[d]		
	Mo···O	1	3.261(23)	0.005(1)[d]		
	Mo···Cu	0.3[e]	3.643(23)	0.008(3)[d]		
	Mo···Cu	0.7[e]	4.230(17)	0.008(3)[d]		
Cu−K-edge	Cu−S	2	2.171(4)	0.008(1)	−11(1)	26.9

[a−d] See Table 1. [e] Constraints for occupancies: *N*(second shell) = 2 − *N*(first shell), *N*(sixth) = *N*(first) − 1, and *N*(seventh) = 1 − *N*(sixth). The partial occupancies of the oxygen shells as well as the related splitting of the Cu shells indicate that the reduction of CODH-H by CO is complete to 70%.

of CODH-H [Figure 2, Table 1 (II)]. The model describes a [CuSMo(═O)$_2$] cluster coordinated by the Sγ of Cys^{388} and the enedithiolates of MCD (Figure 5A). The shorter Mo−S distance of 2.29 Å determined by EXAFS is equivalent to 2.3 Å (*5*) obtained by X-ray crystallography. The distance is considerably longer than 2.15 Å of the double-bonded cyanolyzable sulfur in oxidized, intact xanthine dehydrogenase (*22*). Moreover, it is shorter than the Mo−S_{Cys} bond lengths of 2.41 and 2.5 Å reported for recombinant human sulfite oxidase (*23*) and chicken liver sulfite oxidase (*24*), respectively. Typical bridging Mo−S_b bond lengths in model compounds vary from 2.29 to 2.41 Å (*25*). The average Mo−S distances (sulfide bridge to Fe) in Fe_3MoS_4-containing clusters range from 2.34 to 2.39 Å (*26*). Therefore, the Mo−S bond length of 2.29 Å indicates a bridging function of a single S attached to Mo in CODH-H and provides an argument against a Mo═S or a Mo−S_{Cys} bond. The 2-fold S-coordinated Cu has a distance of 3.70 Å to the Mo. Inspection of the X-ray crystal structure (*4*, *5*) shows that the Sγ of Cys^{388} and the Mo−S are the only potential Cu-coordinating S ligands within a radius of 14 Å from the Mo leading us to postulate the [CuSMo(═O)$_2$] cluster as shown in Figure 5A. From the distances Cu−S = 2.18 Å, Mo−S = 2.29 Å, and Mo···Cu = 3.70 Å, the CuSMo angle can be calculated as 112°. Oxidized CODH-H contains Cu^I and Mo^{VI}, which is apparent from their XANES spectra (Figure

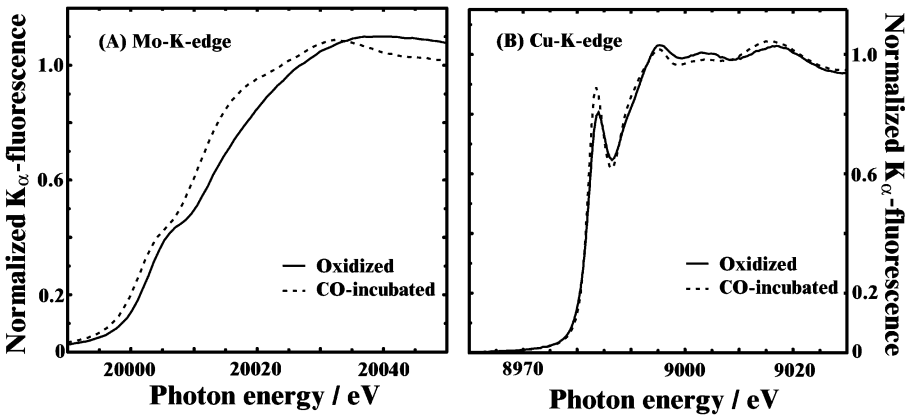

FIGURE 3: Normalized Mo−K-absorption (A) and Cu−K-absorption (B) edges for oxidized (solid lines) and CO-incubated (broken lines) CODH-H.

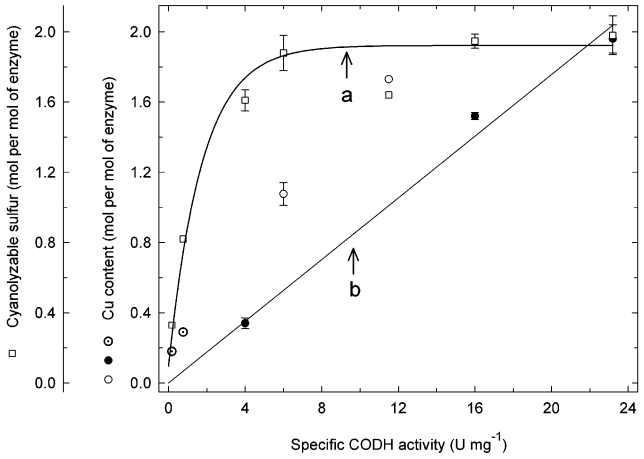

FIGURE 4: Specific CODH activities and contents of Cu and cyanolyzable S in CODH preparations obtained from different CO-grown batches of *O. carboxidovorans*. Analyses of Cu by ICP-AES and of cyanolyzable S as thiocyanate were as detailed in Materials and Methods. Symbols: □, cyanolyzable sulfur content (curve a); ●, ⊙, ○, Cu content. Curve b (●) shows preparations of CODH exhibiting a linear relationship between Cu content and activity. These preparations are composed of CODH species carrying the mature [CuSMo(=O)$_2$] cluster or the immature [HSMo(=O)OH$_{(2)}$] cluster. Dotted circles (⊙) refer to CODH preparations which are incomplete in Cu as well as in cyanolyzable S. Open circles (○) refer to CODH preparations complete in cyanolyzable S and incomplete in Cu which do not show a linear relationship between Cu content and specific CODH activity. They are believed of being composed of three CODH species carrying the mature [CuSMo(=O)$_2$] cluster, the immature [HSMo(=O)OH$_{(2)}$] cluster, and an immature Cu- and S-containing cluster. Error bars were calculated from at least three independent determinations.

3), and has been discussed above. A further backscattering contribution in the Mo−K-edge spectrum corresponds to an O at Mo···O = 3.45 Å, which we attribute to Oϵ1 of Glu^{763} according to the crystal structure (*4*, *5*).

The proposed [CuSMo(=O)$_2$] cluster of Figure 5A agrees with the active site structure revealed by MAD measurements at the Cu−K-edge at high resolution, EPR spectroscopy, and biochemical analyses (*7*). A difference applies to the Mo−O bond length of the equatorial O, which has been determined to 1.74 Å by EXAFS (Table 1) and to 1.87 Å by crystallography (*7*). Whether the difference can be attributed to the different physicochemical conditions apparent in CODH crystals (high salt, presence of 2-methyl-2,4-pentanediol) or CODH solution (low salt, aqueous) must await further studies. The binuclear [Cu^{I}SMo^{VI}(=O)$_2$] cluster of oxidized CODH represents a new type of active site in molybdoenzymes. It is structurally unrelated to the [S$_2$MoS$_2$CuS$_2$MoS$_2$]$^{3-}$ cluster in the "orange protein" of *Desulfovibrio gigas*, a protein of as yet unknown function (*27*).

Reduction by CO Gives Rise to a [Cu^{I}SMo^{IV}(=O)OH$_{(2)}$] Cluster. The effect of the substrate CO on the coordination environment of Cu and Mo in the [CuSMo(=O)$_2$] cluster has been studied by XAS at the Mo− and Cu−K-edges of CODH-H reduced with CO (Figure 6, Table 2).

The Mo−K-edge EXAFS spectrum (Figure 6A) is reproduced by assuming 1.3 O atoms at a distance of 1.70 Å, 0.7 O atom at 2.16 Å, two S atoms at 2.35 Å, and a third S atom at 2.46 Å (Table 2). The Mo−O distance of 2.16 Å allows an assignment as a hydroxy or water ligand (*28*). The contributions at 3.64 and 4.23 Å in the corresponding Fourier transform reflect 0.3 and 0.7 Cu atoms, respectively (Figure 6B). The partial occupancies for the double-bonded oxo ligand and the "splitting" for the Cu backscattering (Table 2) indicate that in CO-treated CODH-H ∼70% of the binuclear centers are reduced, whereas ∼30% remained in the oxidized state. The most prominent differences between the oxidized and reduced clusters are the conversion of one oxo group to a hydroxy or a water ligand, a considerable stretching of the Mo···Cu distance from 3.70 to 4.23 Å, and a change of the symmetric enedithiolate coordination of the Mo in the oxidized [CuSMo(=O)$_2$] center (Figure 5A) into an asymmetric coordination in the reduced [CuSMo(=O)OH$_{(2)}$] state (Figure 5B). The 112° angle ∠(Mo−S−Cu) in [CuSMo(=O)$_2$] increases to 139° in [CuSMo(=O)OH$_{(2)}$]. The Mo−K-edge position for the [CuSMo(=O)OH$_{(2)}$] cluster is at 20001.4 eV (Figure 3A, dotted line) and has shifted about 1.6 eV toward lower energies compared to the [CuSMo(=O)$_2$] center (Figure 3A, solid line). For dimethyl sulfoxide reductase, a shift of 1.9 eV of the Mo−K-edge to lower energy has been interpreted as a reduction of Mo^{VI} to Mo^{IV} (*29*).

The direct Cu coordination environment in CO-treated CODH-H is composed of two S atoms at a Cu−S distance of 2.17 Å (Figure 6D, Table 2). The prominent peak at about 8984 eV in the XANES spectra of oxidized as well as CO-treated samples of CODH (Figure 3B) is typical for a nonlinear, two-coordinate Cu^{I}. This 1s → 4p electronic transition (*19*) is intensified after treatment of CODH-H with CO (Figure 3B), which is ascribed to an increased S−Cu−S

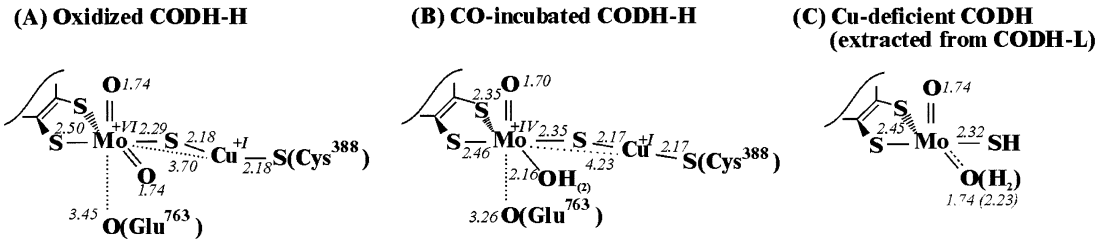

FIGURE 5: Structural models of the active site in CODH derived by XAS: (A) oxidized CODH-H; (B) CO-incubated CODH-H; (C) Cu-deficient species of CODH. The coordination geometry, which usually cannot be determined by XAS, was chosen in analogy to crystallographic data (*4*, *5*).

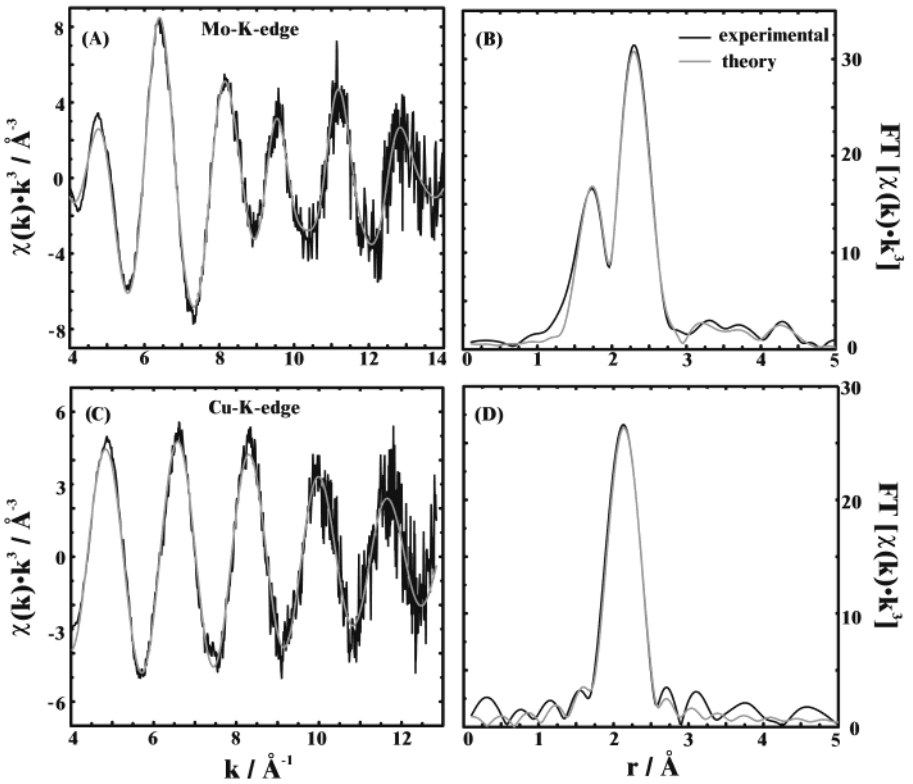

FIGURE 6: Mo−K-edge (A) and Cu−K-edge (C) EXAFS and Fourier transforms (B, D) for CO-incubated CODH-H. Experimental data are depicted as black lines; calculated spectra are represented by gray curves. Parameters are listed in Table 2. For abbreviations see Figure 1.

angle (*19*) in the [CuSMo(═O)$OH_{(2)}$] cluster. The structural model for the [CuSMo(═O)$OH_{(2)}$] cluster in substrate-incubated CODH-H (Figure 5B) results from the combination of the refinements of the Mo− and Cu−K-edge data (Table 2). The models in Figure 5A,B prove the pivotal function of Mo in the structural adjustments upon enzyme reduction. The Mo attracts the ligands −SCu and ═O in the oxidized cluster and relaxes them upon reduction. In addition, the Oϵ1 of Glu^{763} in the oxidized cluster has moved closer toward the Mo in the reduced cluster.

The XAS results demonstrate that Mo is the redox-active metal of the binuclear cluster (Figure 3A). The shift of 1.6 eV in the Mo−K-edge position is consistent with a two-electron transfer to the Mo (*29*). The replacement of the equatorial oxo group in the [CuSMo(═$O)_2$] cluster with a hydroxy or water ligand in the [CuSMo(═O)$OH_{(2)}$] cluster results in a change of the MCD C1′−S−Mo bond length from 2.50 to 2.35 Å upon reduction (trans effect).

Cu-Deficient CODH Contains a [HSMo(═O)$OH_{(2)}$] Center. Depending on growth and physiological conditions *O. carboxidovorans* reveals electrophoretically homogeneous preparations of CODH which are composed of active and inactive CODH species. Figure 4 shows that CODH preparations with specific activities ranging from about 4 to 23.2 units mg^{-1} are complete in bridging S (Figure 4, curve a) and incomplete in Cu, whereas in enzyme preparations of less than about 4 units mg^{-1} Cu and bridging S are substoichiometric and low. The three preparations examined here (23 units mg^{-1}, CODH-H; 16 units mg^{-1}, CODH-M; 4 units mg^{-1}, CODH-L) show a linear relationship of activity and Cu content (Figure 4, curve b), which characterizes them as two-component mixtures of the active [CuSMo(═$O)_2$] enzyme species and an inactive Cu-deficient species. Two preparations (6.0 and 11.5 units mg^{-1}) show higher Cu contents than suggested by the specific enzyme activities (Figure 4), referring to the existence of precursors in the biosynthesis of the metal cluster which are immature although they contain Cu and S. To study the structure of the Cu-deficient active site by Mo−K-edge XAS, the CODH-L preparation was chosen because its activity (4 units mg^{-1} compared to 23.2 units mg^{-1} CODH-H) and Cu content (0.34 mol compared to 1.96 mol per mole of enzyme) indicate a mixture of 17% active [CuSMo(═$O)_2$] CODH and of 83% inactive Cu-deficient CODH.

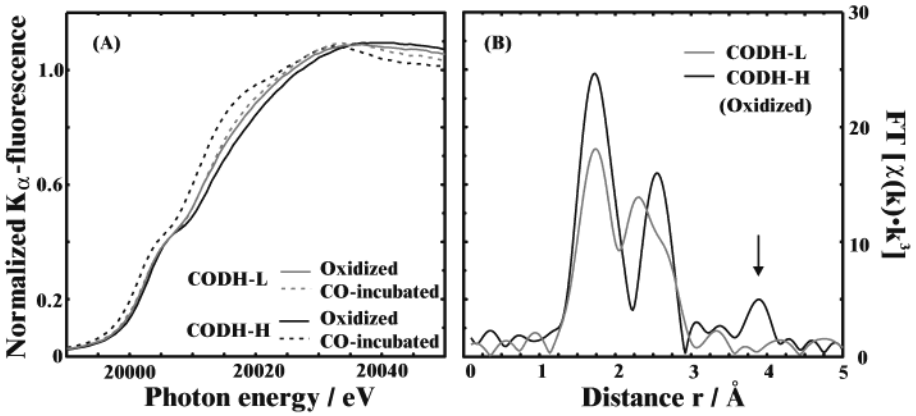

FIGURE 7: (A) Normalized Mo−K-edges of oxidized (solid lines) and CO-incubated (broken lines) CODH-L (gray) and CODH-H (black). (B) Fourier transformed Mo−K-edge EXAFS of oxidized CODH-L and CODH-H. For abbreviations see Figure 1.

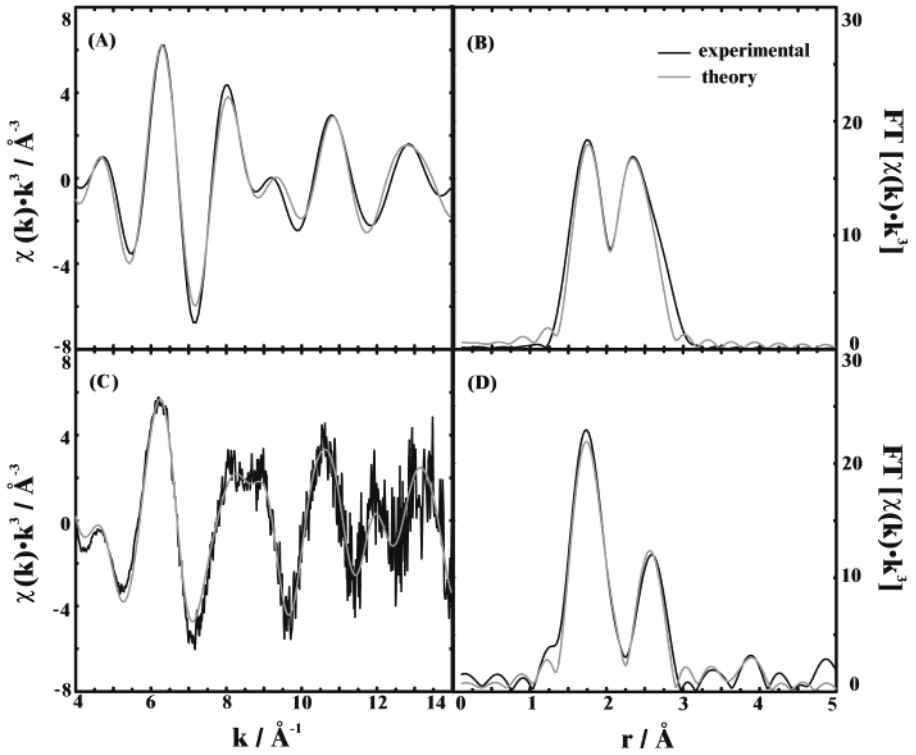

FIGURE 8: Mo−K-edge EXAFS (A, C) and Fourier transforms (B, D) of Cu-deficient CODH and CODH-M. Experimental (black lines) and calculated (gray lines) data are coplotted. (A, B) Fourier-filtered spectrum (1.2−3 Å) and corresponding Fourier transform of the inactive form of CODH, extracted from CODH-L: [(spectrum CODH-L) − 0.17(model CODH-H)]/0.83. Parameters are listed in Table 3. (C, D) Reproduction (gray line) of the experimental EXAFS and corresponding Fourier transform of CODH-M: 0.7(model CODH-H) + 0.3(model inactive species). The value for the Fermi energy E_F was constrained to a value calculated according to the same equation. For abbreviations see Figure 1.

The functionality of the Mo site in CODH was monitored by measuring the Mo edge shift upon CO incubation for different species (Figure 7A). CODH-H, carrying the [CuSMo] cluster, exhibits the expected edge shift of more than 1.5 eV and is therefore considered to be fully active. In contrast, the lack of a considerable edge shift for CODH-L reflects its large content of inactive species, which we assume to be 83% (assuming CODH-H to be fully active) according to activity and Cu content (Figure 4).

The Fourier-transformed Mo EXAFS of CODH-L exhibits no significant backscattering contributions at distances exceeding 3 Å. In particular, the Cu contribution corresponding to the 17% active CODH species in the CODH-L preparation expected at 3.70 Å could not be separated from the noise level (Figure 7B, arrow). The EXAFS of the inactive fraction of CODH-L (Figure 8A,B) was obtained by subtracting 17% of modeled CODH-H [Table 1 (I)] from the EXAFS of the CODH-L preparation. The resulting difference spectrum was normalized, and the noise level was reduced by Fourier filtering, retaining only significant contributions (1.2−3 Å).

The first coordination sphere of Mo in the inactive species contains O- and S-substituents (Table 3) arranged as a Cu-deficient [HSMo(=O)$OH_{(2)}$] center (Figure 5C). The single S atom at 2.32 Å was modeled as −SH (*22*). The two S atoms at 2.45 Å were interpreted as the enedithiolates of MCD. The 1.4 O atoms at 1.74 Å were modeled as oxo groups, and the 0.6 O atom at 2.23 Å was interpreted as

Table 3: EXAFS Refinement Parameters for Cu-Deficient CODH (Extracted from CODH-L)[a]

model	atom	*N*	*r*/Å	$2\sigma^2$/Å^2	E_F[b]/eV	*R*[c]/%
Mo−K-edge	Mo═O	1.4(2)	1.738(5)	0.003(1)[d]	−16(2)	21.4
	Mo−O	0.6[e]	2.230(14)	0.003(1)[d]		
	Mo−S	1	2.316(16)	0.008(2)[d]		
	Mo−S	2	2.453(19)	0.008(2)[d]		

[a−d] See Table 1. [e] Constraints for occupancies: *N*(second shell) = 2 − *N*(first shell). The noninteger occupancies of the oxygen shells suggest partial protonation of an oxo group as indicated in Figure 5C.

water (*28*). Apart from the presence or absence of Cu, the average Mo coordination environments in active CODH-H and inactive, Cu-deficient CODH are very similar (2 O, 3 S ligands), demonstrating that Cu is an essential constituent of a functional active site.

Moreover, the data suggest that CODH-L and CODH-M represent two-component mixtures of the active enzyme species, containing the [CuSMo(═O)$_2$] cluster (Figure 5A) and an inactive species that is depleted of Cu (Figure 5C). This is verified by examination of CODH-M, which has about 70% of the maximum enzyme activity. The experimental EXAFS spectrum (Figure 8C, black curve) and the corresponding Fourier transform (Figure 8D, black curve) could be fully reproduced (Figure 8C,D, gray curves) by adding the models corresponding to 70% of the [CuSMo(═O)$_2$] cluster and 30% of the [HSMo(═O)OH$_{(2)}$] center. The quality of the reproduction is apparent from the fact that no single parameter has been refined.

The functional and the nonfunctional species of CODH are modifications of the same enzyme present in *O. carboxidovorans* and copurify upon protein preparation. Current mutational studies suggest that the nonfunctional Cu-deficient CODH species is a precursor in the posttranslational biosynthesis of the [CuSMo(═O)$_2$] cluster encoded by the *coxDEFG* gene cluster. The gene cluster resides on the plasmid pHCG3 of *O. carboxidovorans* and is located immediately transcriptionally downstream of the *coxMSL* CODH structural gene cluster, suggesting functional relationships (*5*, *30*). We have been able to inactivate each gene of the *coxDEFG* cluster by insertion of a kanamycine resistance casette. The CODH species purified from the mutants *coxD:Km* and *coxE*:*Km* were nonfunctional and contained the Mo ion coordinated by the MCD cofactor, and Cu was below the detection limit of the chemical analyses employing 2,2′-bis(quinoline)-4,4′-dicarboxylic acid (BCA). Chemical analyses and a rhombic desulfo-Mo EPR signal established the absence of cyanolyzable S in the nonfunctional CODH species synthesized by the *coxD* mutant. Figure 4 indicates a preparation of wild-type CODH showing a CO-oxidizing activity of 0.17 unit mg^{-1} which was very low in both Cu (0.18 mol/mol of CODH) and cyanolyzable S (0.33 mol/mol of CODH), contained Mo-MCD, and revealed a desulfo-Mo EPR signal. Because the active site composition of the nonfunctional wild-type CODH was similar to that of the CODH species from the *coxD:Km* mutant, we conclude it is a precursor in the posttranslational maturation of the bimetallic center. The nonfunctional CODH from the *coxE* mutant was complete in cyanolyzable S, but Cu was absent. We take this as evidence for a function of the CoxD protein in the attachment of the sulfane sulfur to the active site. Cu was also absent in the nonfunctional *coxF* mutant CODH but was present in the *coxG:Km* CODH which was functional in CO oxidation. This led us to conclude that the proteins CoxE and CoxF have functions in the posttranslational processing of Cu. The similarity of the metal site in the *coxE:Km* mutant CODH species and of the Cu-deficient [HSMo(═O)OH$_{(2)}$] center shown in Figure 5C indicates that the Cu-deficient CODH species present in the CODH-L preparation also is a precursor in the biosynthesis of the bimetallic center.

Conclusions. The bimetallic [CuSMo(═O)$_2$] cluster present in the active site of CODH is the first example for the combination of these two metals in a single catalytically active unit. Also unique is the μ_2-S atom bridging both metals and the coordination of the cluster by the enedithiolate group of MCD at the Mo site and by Cys^{388} at the Cu site. The orange protein of unknown function from *D. gigas* accommodates a $[S_2MoS_2CuS_2MoS_2]^{3-}$ mixed metal−sulfide cluster containing Mo and Cu (*27*). Although both clusters are built up from the same constituents (Mo, Cu, and S), they are structurally unrelated since the former is binuclear and the latter is trinuclear. In addition, Cu and Mo in the [CuSMo(═O)$_2$] cluster are bridged by a single μ_2-S atom whereas two such bridges exist between the metal pairs in the $[S_2MoS_2CuS_2MoS_2]^{3-}$ cluster. The Cu is coordinated by two S in the [CuSMo(═O)$_2$] cluster but tetrahedrally by four S in the $[S_2MoS_2CuS_2MoS_2]^{3-}$ cluster. The [CuSMo(═O)$_2$] cluster of CODH is also unrelated to the Cu site of the blue copper proteins, e.g., poplar plastocyanin, which have the metal coordinated in a distorted tetrahedral site with one cysteine, two histidines, and a methionine providing the ligands (*31*).

The positions of the absorption edges (Figure 3) determine the metal oxidation states in air-oxidized CODH (Mo^{VI} and Cu^{I}) and reduced CODH (Mo^{IV} and Cu^{I}). Moreover, air-oxidized CODH is silent in Mo EPR, but titration with sodium dithionite generates a Mo^{V} EPR signal indicating a +VI oxidation state of Mo in the oxidized enzyme (*7*). CODH in the air-oxidized state or after reduction with dithionite or CO does not reveal a paramagnetic Cu^{II} EPR signal (*7*). However, after wet ashing with hydrogen peroxide in sulfuric acid, which destroys the integrity of the enzyme, a Cu^{II} EPR signal is generated (*7*). This is consistent with our report suggesting a permanent +I oxidation state of the Cu. The Mo ion represents the redox active center and is the likely coordination site for the oxygen atom transferred during the reaction. It is known that Cu^{I} is able to form copper carbonyls and that CO can be reversibly fixed by Cu^{I} solutions (*32*). Thus, we postulate that Cu is involved in substrate binding. Experiments to reconstitute the [CuSMo(═O)$_2$] cluster in nonfunctional CODH by treatment with sodium sulfide plus dithionite plus Cu^{I} thiourea led to 28% reactivation but are not yet conclusive.

The term "mononuclear molybdenum enzymes" has been used to separate those molybdoenzymes in which the metal is coordinated by molybdopterin or one of the various molybdopterin dinucleotides from nitrogenases (*33*). The mononuclear molybdoenzymes have been grouped into three families, the xanthine oxidase family (LSMoO-possessing enzymes), the sulfite oxidase family (LMoO$_2$-possessing enzymes), and the DMSO reductase family (L$_2$MoX-possessing enzymes). According to these categories CODH establishes the new family of binuclear molybdoenzymes (L′CuSMoOL″-possessing enzymes). It is apparent that the

[SMoO] site of the enzymes constituting the mononuclear xanthine oxidase family is part of the [CuSMo(=O)$_2$] cluster of the binuclear CODH's. The presumed evolutionary relationship between the two molybdoenzyme families is also evident from conserved primary amino acid sequences, similar cofactor composition, and quarternary structures (*1*, *4*). The structural relationship of CO and related compounds such as cyanides, isocyanides, N_2, NO^+, azide, or acetylenides can be taken as an indication that probably other homologues of Mo enzymes will be shown to have Cu associated with them.

Finally, it is interesting to note that the CODH from the anaerobic bacterium *Carboxydothermus hydrogenoformans* accommodates a [Ni-4Fe-5S] cluster in which a bimetallic Fe−S−Ni substructure represents the likely site of CO oxidation (*34*). Thus, oxidation of the highly symmetric and nonpolar substrate CO seems to require a mechanism involving a binuclear metal center.

ACKNOWLEDGMENT

We thank Brenda Kostelecky (EMBL, Hamburg Outstation, Germany) and Holger Dobbek (Max Planck Institute of Biochemistry, Martinsried, Germany) for reading the manuscript and Andreas Vogel (EMBL, Hamburg Outstation, Germany) for fruitful discussions.

REFERENCES

1. Schübel, U., Kraut, M., Mörsdorf, G., and Meyer, O. (1995) *J. Bacteriol. 177*, 2197−2203.
2. Mörsdorf, G., Frunzke, K., Gadkari, D., and Meyer, O. (1992) *Biodegradation 3*, 61−82.
3. Meyer, O., and Schlegel, H. G. (1979) *J. Bacteriol. 137*, 811−817.
4. Dobbek, H., Gremer, L., Meyer, O., and Huber, R. (1999) *Proc. Natl. Acad. Sci. U.S.A. 96*, 8884−8889.
5. Meyer, O., Gremer, L., Ferner, R., Ferner, M., Dobbek, H., Gnida, M., Meyer-Klaucke, W., and Huber, R. (2000) *Biol. Chem. 381*, 865−876.
6. Gremer, L., Kellner, S., Dobbek, H., Huber, R., and Meyer, O. (2000) *J. Biol. Chem. 275*, 1864−1872.
7. Dobbek, H., Gremer, L., Kiefersauer, R., Huber, R., and Meyer, O. (2002) *Proc. Natl. Acad. Sci. U.S.A.* (in press).
8. George, G. N., Hedman, B., and Hodgson, K. O. (1998) *Nat. Struct. Biol. 5*, 645−647.
9. Meyer-Klaucke, W., and Strange, R. W. (2000) *Synchrotron Radiat. News 13*, 17−21.
10. Kraut, M., Hugendieck, I., Herwig, S., and Meyer, O. (1989) *Arch. Microbiol. 152*, 335−341.
11. Meyer, O., and Rajagopalan, K. V. (1984) *J. Biol. Chem. 259*, 5612−5617.
12. Westley, J. (1981) *Methods Enzymol. 77*, 285−291.
13. Stern, E. A., and Kim, K. (1981) *Phys. Rev. B23*, 3781−3787.
14. Pettifer, R. F., and Hermes, C. (1985) *J. Appl. Crystallogr. 18*, 404−412.
15. Nolting, H. F., and Hermes, C. (1992) EXPROG: EMBL EXAFS data analysis and evaluation program package.
16. Binsted, N., Strange, R. W., and Hasnain, S. S. (1992) *Biochemistry 31*, 12117−12125.
17. Eidsness, M. K., Scott, R. A., Prickril, B. C., DerVartanian, D. V., Legall, J., Moura, I., Moura, J. J. G., and Peck, H. D., Jr. (1989) *Proc. Natl. Acad. Sci. U.S.A. 86*, 147−151.
18. Meyer, O. (1982) *J. Biol. Chem. 257*, 1333−1341.
19. Kau, L., Spira-Solomon, D. J., Penner-Hahn, J. E., Hodgson, K. O., and Solomon, E. I. (1987) *J. Am. Chem. Soc. 109*, 6433−6442.
20. Pickering, I. J., George, G. N., Dameron, C. T., Kurz, B., Winge, D. R., and Dance, I. G. (1993) *J. Am. Chem. Soc. 115*, 9498−9505.
21. Mijovilovich, A., and Meyer-Klaucke, W. (2001) *J. Synchrotron Radiat. 8*, 692−694.
22. Cramer, S. P., Wahl, R., and Rajagopalan, K. V. (1981) *J. Am. Chem. Soc. 103*, 7721−7727.
23. George, G. N., Garrett, R. M., Prince, R. C., and Rajagopalan, K. V. (1996) *J. Am. Chem. Soc. 118*, 8588−8592.
24. Kisker, C., Schindelin, H., Pacheco, A., Wehbi, W. A., Garrett, R. M., Rajagopalan, K. V., Enemark, J. H., and Rees, D. C. (1997) *Cell 91*, 973−983.
25. Cramer, S. P., Hodgson, K. O., Gillum, W. O., and Mortenson, L. E. (1978) *J. Am. Chem. Soc. 100*, 3398−3407.
26. Stiefel, E. I. (1980) in *Molybdenum and molybdenum-containing enzymes* (Coughlan, M. P., Ed.) pp 41−98, Pergamon Press Ltd., Oxford, U.K.
27. George, G. N., Pickering, I. J., Yu, E. Y., Prince, R. C., Bursakov, S. A., Gavel, O. Y., Moura, I., and Moura, J. J. G. (2000) *J. Am. Chem. Soc. 122*, 8321−8322.
28. Romão, M. J., Rösch, N., and Huber, R. (1997) *J. Biol. Inorg. Chem. 2*, 782−785.
29. Baugh, P. E., Garner, C. D., Charnock, J. M., Collison, D., Davies, E. S., McAlpine, A. S., Bailey, S., Lane, I., Hanson, G. R., and McEwan, A. G. (1997) *J. Biol. Inorg. Chem. 2*, 634−643.
30. Santiago, B., Schübel, U., Egelseer, C., and Meyer, O. (1999) *Gene 236*, 115−124.
31. Redinbo, M. R., Yeates, T. O., and Merchant, S. J. (1994) *J. Bioenerg. Biomembr. 26*, 49−66.
32. Pasquali, M., and Floriani, C. (1983) in *Copper Coordination Chemistry: Biochemical and Inorganic Perspectives* (Karlin, K. D., and Zubieta, J., Eds.) pp 311−330, Adenine Press, Guilderland, NY.
33. Hille, R. (1996) *Chem. Rev. 96*, 2757−2816.
34. Dobbek, H., Svetlitchnyi, V., Gremer, L., Huber, R., and Meyer, O. (2001) *Science 293*, 1281−1285.

BI026514N